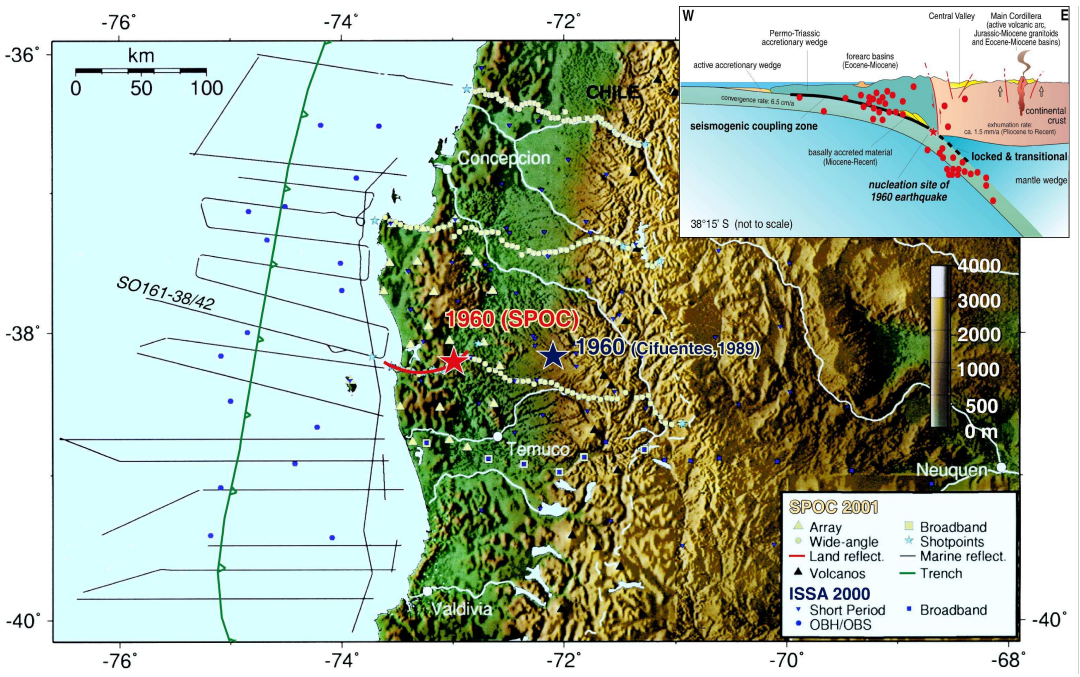

Figure 4.15: Map of the investigation area with locations of the SPOC profiles (from Krawczyk and the SPOC Team (2003)). The blue asterisk marks the epicenter location of the 1960 Valdivia earthquake from Cifuentes (1989), the red asterisk indicates the relocated epicenter position suggested by Krawczyk and the SPOC Team (2003). The inset illustrates a schematic conceptual model of the crustal structure of the southern Chilean subduction zone at 38° 15′S.

4.3 The Southern Andes

The SPOC (Subduction Processes off Chile) project investigated the subduction zone of the Southern Andes between 36° and 40° S. A large number of seismic on- and offshore profiles were acquired to study the fore-arc region and the seismogenic coupling zone of the active accretionary margin (see Fig. 4.15). One of the data sets that provided a detailed image of the near coastal subduction zone is the near-vertical reflection profile (SPOC-NVR) (red line in Fig. 4.15). The results of prestack depth migration and the application of RIS to the NVR data are presented in the following.

4.3.1 The investigation area

Compared to the Central Andes the Southern Andes are a low-relief mountain belt with maximum elevations of about 3000 m. The mountain belt is about 300 km wide (E-W)

and the crustal thickness below the magmatic arc is about 35 - 40 km (Lüth et al., 2003b; Bohm et al., 2002). These dimensions are small compared to the Central Andes, where the mountain belt is about 800 km wide and the crustal thickness is about 60 - 70 km (Rosenau, 2004; Beck et al., 1996). In the investigation area near Valdivia the largest earthquake ever recorded occurred in the year 1960 with a magnitude of 9.5. Its epicenter was located at 30 - 40 km depth below the fore-arc. The estimated rupture length of this earthquake was about 1000 km, the vertical displacement was up to 2 m and the co-seismic slip 40 m, respectively (Cifuentes, 1989; Kanamori and Cipar, 1974; Plafker and Savage, 1970). The epicenter location of this earthquake after Cifuentes (1989) is marked by the blue asterisk in Fig. 4.15. Krawczyk and the SPOC Team (2003) suggested a relocated epicenter of the earthquake from the seismic reflection image (red asterisk in Fig. 4.15).

The morphostructural units of the Southern Andes are the Coastal Cordillera, the Longitudinal Valley and the Main Cordillera (see Fig. 4.16). The **Coastal Cordillera**, with its highest elevations around 1500 m, can be separated into two lithological units: the Western and the Eastern Series (Hervé, 1977). The basement of the Western Series is a tectonic mélange that consists of metamorphic rocks and serpentinites (Rosenau, 2004). Greenschist to bluschist facies in this unit indicate high-pressure and low-temperature conditions during the metamorphosis (Willner et al., 2001, 2003). This unit is interpreted as the basal part of the Permotriassic accretionary wedge (Aguirre et al., 1972). In the Eastern Series greenschist to granulite facies indicate low-pressure and high-temperature conditions in the metamorphic history (Hervé, 1977). This area is interpreted as the Permocarbonifereous magmatic arc (Martin et al., 1999). NE-SW trending lineaments related to Triassic rifting and NW-SE lineaments from Permotriassic foliation and thrusts of the paleo-accretionary wedge are characteristic for the Coastal Cordillera (Muñoz, 1997; Hervé, 1977). Volcanic rocks and marine and nonmarine sediments of the Tertiary age and Quarternary sediments cover the Coastal Cordillera and the **Longitudinal Valley** to the east. The intrusion of the North Patagonian Batholith during the Meso-Cenozoic built up the **Main Cordillera** (Hervé, 1994). The present magmatic arc is a ca. 200 km wide mountain belt with average heights of about 1000 m. A chain of andesitic to basaltic stratovolcanoes are located in the Main Cordillera (Lüth et al., 2003b).

4.3.2 The SPOC-NVR profile

In 2001 the SPOC-NVR profile was acquired near the coast at 38°15′ S (Fig. 4.15). It was carried out as a combined offshore-onshore reflection seismic experiment consisting of three spreads containing 180 geophones each. The geophone spacing was 100 m. A

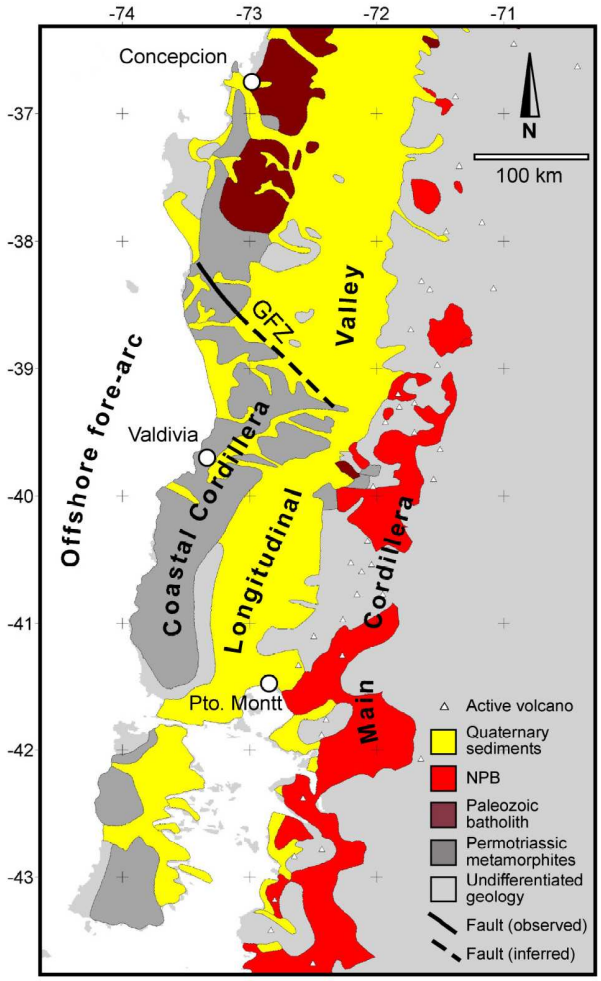

Figure 4.16: Tectonic units and simplified geology of the Southern Andes (from Rosenau (2004)). GFZ = Gastre Fault Zone, NPB = North Patagonian Batholith.

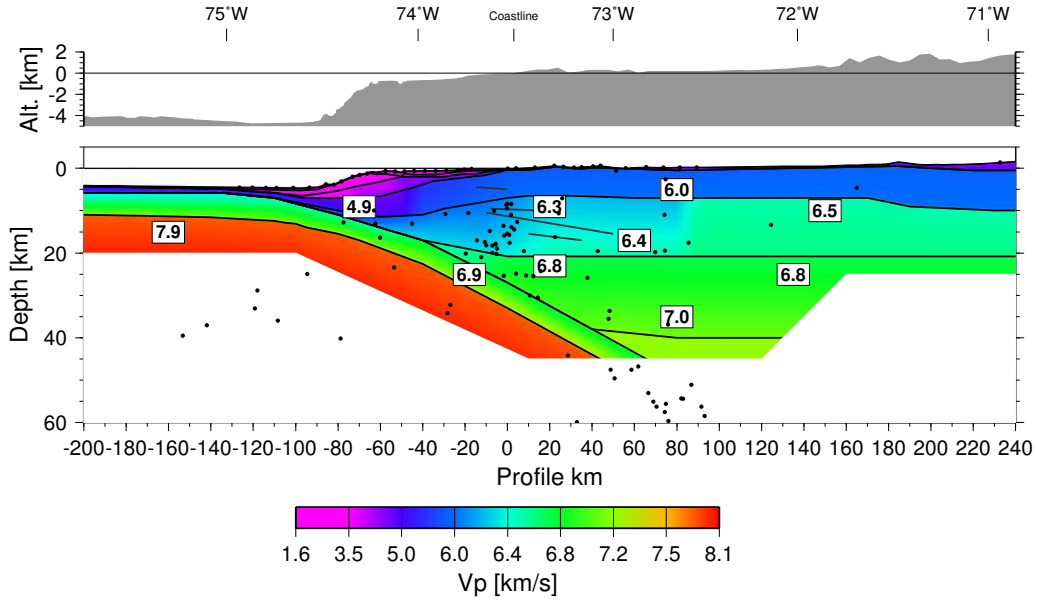

Figure 4.17: Velocity model SPOC from refraction data analysis (Lüth et al., 2003a) with black dots indicating hypocenter locations (Bohm et al., 2002).

total of 14 shots at 10 different locations were recorded (Fig. 4.18). The 54 km long E-W oriented crooked line profile had a CMP fold of 1-2. The total recording time of each shot gather was 25 s, the sampling rate was 5 ms.

Kirchhoff prestack depth migration

The shot gathers were band-pass filtered (5 - 30 Hz). A time variant shift of the signal (1 Hz) caused by instrument amplifier drift was removed (DC shift removal). Trace editing and muting of bad traces was applied to suppress additional migration noise. The geometrical spreading was corrected and air-blasts were muted. Top and bottom muting were applied to suppress the first arrivals and strong noise at later arrival times.

The migration was performed in 3D. A wide-angle experiment was carried out simultaneously in the same area and the analysis of the obtained refraction data provided the velocity model for the depth migration (Lüth et al., 2003a).The velocity model used for migration is shown in Fig. 4.17. Under the assumption that the variations of the velocities perpendicular to the profile were small, the 2D model was stretched in N-S direction, thus providing a 2.5D model. The travel time calculations, the migration and the stacking

schemes were implemented in the same way as for the ANCORP data set (see section 4.2.2). The x-, y-, and z-axis for travel time calculation and migration corresponded to W-E, N-S direction and depth, respectively (Fig. 4.18).

The travel times were calculated from topography using a FD-eikonal solver (see section 3.1.3). For each source and receiver location travel time tables were computed containing the travel times from the surface to each grid point of a 100 km $\times$ 24 km $\times$ 60 km large subsurface volume. The final migration volume was 200 km $\times$ 24 km $\times$ 60 km. The grid spacing in x-, y- and z-direction was 200 m $\times$ 2000 m $\times$ 40 m, respectively. To avoid migration noise near the surface a dip mute was applied at far-offsets during migration. After migration of the single shot gathers selected depth slices of the 3D migrated section were stacked together (Fig. 4.18). This so-called offline stacking of parallel E-W oriented depth slices located near the profile line provided the final 2D depth sections. The offline stacking was preformed using different schemes to improve the signal-to-noise ratio. The following schemes were used:

1. phase stacking, i.e. stacking of the migrated single sections.

2. stacking of absolute amplitudes, i.e. the absolute amplitudes of the migrated single sections were calculated and stacked.

3. envelope stacking, i.e. the depth trace envelopes of the migrated single sections were calculated and stacked.

4. stacking of normalised envelope sections, i.e. the trace envelopes of the migrated single sections were calculated, the envelope sections were normalised to the maximum amplitude in each section, and the normalised sections were stacked.

5. envelope stacking and additional normalisation of the sections to the maximum amplitude of each trace. Additionally, the traces of the final section were normalised to the maximum amplitude in each trace.

The comparison of the stacked sections showed that stacking scheme 2 and scheme 5 provided the optimum results i.e. comparatively the lowest signal-to-noise ratio and the most dictinct reflections in the image. Obviously, the data are sensitive to the stacking process, due to the low data coverage, the low signal-to-noise ratio and the different amplitude levels in the records. In the following only the results from stacking scheme 2 and scheme 5 will be presented and discussed.

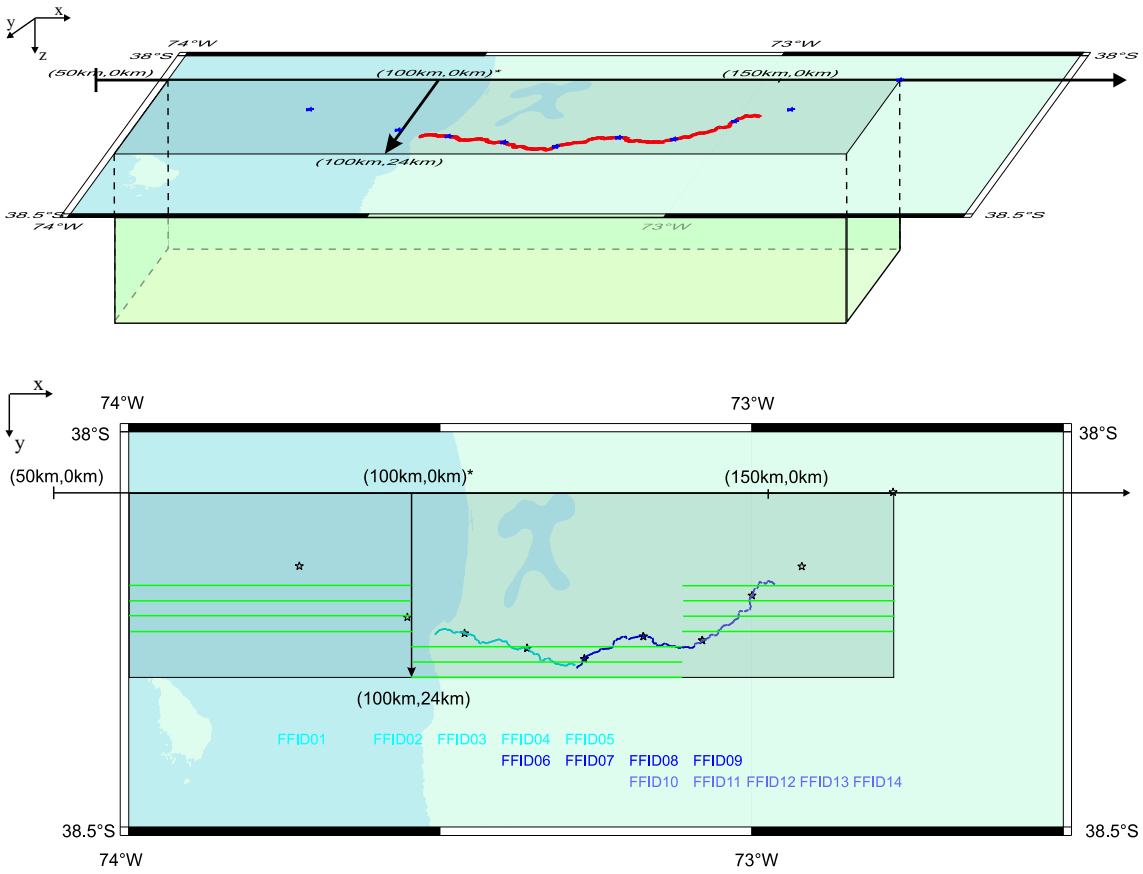

Figure 4.18: Schematic view of the migration geometry. **Top:** 3D view of the migration volume and the profile location (red line). The shot point locations are indicated by blue asterisks. **Bottom:** Top view of the local coordinate system. The colours indicate the shot points and the corresponding receiver arrays (Blue: FFID 01 - 05 recorded by the first array; Dark purple: FFID 06 - 09 recorded by the second array; Light purple: FFID 10 - 14 recorded by the third array). The green lines indicate the E-W depth slices that were stacked yielding the final 2D depth sections.